SEMARAK ILMU PUBLISHING

Journal of Advanced Research in Applied Mechanics

Journal homepage:
https://semarakilmu.com.my/journals/index.php/appl_mech/index
ISSN: 2289-7895

Polarization Curve of Chloride-Induced Corrosion in Steel Using a Three-Dimensional Model

Suhaila Salleh[1,2,*], Noor Mirza Syamimi Mortadha[1], Alzakri Ekhwan[3]

[1] Fakulti Kejuruteraan Mekanikal, Universiti Teknikal Malaysia Melaka, Hang Tuah Jaya, 76100 Durian Tunggal, Melaka, Malaysia
[2] Centre for Advanced Research on Energy, Universiti Teknikal Malaysia Melaka, Hang Tuah Jaya, 76100 Durian Tunggal, Melaka, Malaysia
[3] Mechanical Section, Engineering Department, Group Technical Solutions Project Delivery & Technology (PD&T), Petroliam Nasional Berhad (PETRONAS), 50088 Kuala Lumpur, Malaysia

ARTICLE INFO

Article history:
Received 5 February 2023
Received in revised form 25 April 2023
Accepted 1 May 2023
Available online 16 May 2023

Keywords:
Corrosion; steel; model

ABSTRACT

Corrosion process occurs naturally in which metals, such as steel, undergo degradation due to chemical or electrochemical reactions with their surroundings. This however can lead to serious malfunctions and costly damages to crucial steel uses. In marine activities, most metals and alloys used inevitably degrade since the sea is rich in corrosive electrolytes, in particular, chloride. This may lead to the occurrence of pitting corrosion, which is highly localised and can cause major catastrophes. Hence, it is important to understand the science of pitting corrosion which in turn can benefit corrosion control processes. This can be done through simulation of pitting activities. In this study, a three-dimensional model of a minute pit in steel, immersed in sodium chloride solution in water, is simulated using COMSOL Multiphysics version 5.6 with Chemical Reaction Engineering Module. The simulation is run to observe the shape of the polarization curve at the actively corroding pit. The initial pH of the immersing solution is at a slightly alkaline condition, namely at pH 8. The results show that the corrosion potential, E_{corr}, of a point at the bottom of the corroding pit is -0.74 V. The model is also able to show a high concentration of ferrous ions, Fe^{2+}, inside the pit geometry, reaching to a value of 2.5×10^{3} mol m^{-3}. These results indicates that metal dissolution occurs. The shape of the polarization curve obtained in this study exhibits a significant linkage to the propagation of pit, which in turn indicates the type of corrosion a pit can evolve into, in particular, pitting corrosion.

1. Introduction

Corrosion is a process of material destruction that often occurs in metallic materials when exposed to a corrosive environment. This phenomenon induces an aggressive type of localized corrosion called pitting corrosion [1]. Studies have been done on different types of metal to look at the corrosion rate when pitting corrosion occurs [2]. However, to understand the corrosion rate, one needs to understand the science of corrosion, which is the heart of this research.

* *Corresponding author.*
E-mail address: suhaila@utem.edu.my

https://doi.org/10.37934/aram.106.1.2736

Corrosion can be categorized into two types, namely uniform and local corrosion. Local or localized corrosion occurs at a particular region on the metal surface while uniform corrosion grows uniformly [3].

When steel is exposed to a solution of sodium chloride (NaCl), such as seawater, it can undergo accelerated corrosion due to the highly corrosive nature of this environment. The mechanism of localized corrosion starts with the disintegration or weakening of the surface layer, and progresses to the slow attack of chloride ions on a very particular and tiny area on the metal surface [4]. The corrosion process in steel in sodium chloride solution can be described as an electrochemical reaction which involves the anodic dissolution of iron and the cathodic reduction of oxygen or hydrogen ions. Iron dissolution leads to the formation of ferrous ions, Fe^{2+}, and the release of electrons, while the reduction of oxygen or hydrogen ions leads to the formation of hydroxide ions, OH^- [5].

The science of corrosion has been studied through modelling, with validation using published results. However, the initiation of pits on metal surfaces has yet to be fully understood [6]. A two-dimensional axial-symmetric model has been studied to investigate the propagation of pit, after the initiation state [7]. Many factors can influence the rate of corrosion of steel in sodium chloride solution, including the concentration of chloride ions, the pH of the solution, the temperature, and the presence of other contaminants or impurities [8]. In a recent study, steel in weak-alkaline chloride solution is used to study a type of localized corrosion, which is pitting [9]. The aim of this study is to construct a three-dimensional model in COMSOL Multiphysics version 5.6 software and set the initial pH of the immersing liquid surrounding the metal to be slightly alkaline, which is of pH 8. The expected result is to obtain the polarization curve, which is the graph of the current density versus the electrode potential, for all stated initial pH values to predict the evolution of the corroding metal surface at higher potential.

2. Methodology

A three-dimensional model geometry is constructed in COMSOL Multiphysics, as in Figure 1. The curved region is set as the active boundary, representing the active metal surface. The box-like region at the top of the geometry is set as the bulk solution. However, the surface in touch with the active pit is set as an inactive region. Activities at the active and inactive regions are studied by plotting graphs at the points 6 and 5, respectively.

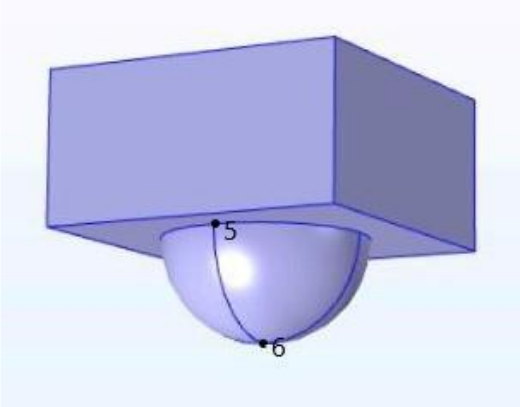

Fig. 1. Geometry structure of the three-dimensional model

Electrochemical reactions involved in the corrosion activities of a corroding steel surface are studied to set the ionic species to be considered in the model. A set of mathematical equations is used to simulate the mass transport of the ionic species. The eleven ionic species are

i. Chloride ion, Cl^-
ii. Sodium ion, Na^+
iii. Metal ion from dissolution process, Fe^{2+}
iv. Iron (II) monohydroxide ion, $FeOH^+$
v. Hydrogen ion, H^+
vi. Hydroxyl ion, OH^-
vii. Iron (II) chloride ion, $FeCl^+$
viii. Ferric ion, Fe^{3+}
ix. Iron oxide ion, FeO_2^-
x. Iron oxyhydroxide ion, $HFeO_2^-$
xi. Iron (II) chloride ion, $FeCl^{2+}$

The behavior of these ionic species can be represented by a governing equation called the Nernst-Planck equation [10-12].

$$\frac{\partial[i]}{\partial t} = D_i\nabla^2[i] + z_iU_iF\nabla([i]\nabla V) + R_i \quad (1)$$

where $[i]$ is the concentration of species *i*

i. D_i is the effective diffusion coefficient
ii. z_i is the charge number
iii. U_i is the mobility (given that U_i=$\frac{Di}{RT}$)
iv. R_i is the rate of production/depletion of *i*
v. ∇V is the potential gradient

This equation considers the diffusion and migration of species, combined with the electroneutrality to describe the electrolyte during corrosion process.

In the context of corrosion, current density is often used to describe the rate of electrochemical reactions that contribute to the corrosion process, such as the oxidation or reduction of metal ions. To obtain the polarization curve, the corrosion current densities at the interface are studied through the contributions of the anodic and cathodic reactions. The corrosion rate, or the speed at which the corroding activities happen, is measured by corrosion kinetics. Corrosion kinetics refers to the study of the mechanism and rate of the corrosion process which includes the occurrences of various chemical and electrochemical reactions.

Current density, $i = i_a - i_c = i_{corr}(\exp\left(\frac{n}{\beta_a}\right) - \exp\left(\left(\frac{-n}{\beta_c}\right)\right)$ (2)

where i_a is the anodic current

i. i_c is the cathodic current.
ii. n is the overpotential at metal surface
iii. β_a is the Tafel Coefficient for anodic reaction.
iv. β_c is the Tafel Coefficient for cathodic reaction.

The equation below demonstrates how pH is represented:

$$\text{pH} = -\log_{10}(0.001 \times \text{abs}[\text{H}^+]) \quad (3)$$

where $[H^+]$ is the concentration of hydrogen ions. Due to the conversion from dm^3 to m^3, the concentration term inside the bracket is amplified by 0.001. In order to vary the initial pH value of the bulk solution, the initial concentration of H^+ was changed, as shown in Table 1 below:

Table 1
The calculation of initial pH using $[H^+]$

pH	$[H^+]$, mol m^{-3}
8	1×10^{-5}
10	1×10^{-7}
12	1×10^{-9}

Corrosion activities involve the fluxes of ionic species. Both the anodic and cathodic fluxes are applied to the active part of the pit geometry [5]. According to Fick's First Law of Diffusion, the current densities for oxidation of iron and proton reduction produce their respective fluxes [13]. The equations of these fluxes are stated as below

Flux of metal ions Fe^{2+}, $J_{diss} = \frac{i1}{2F} = \frac{0.25\ x\ i01}{F} \exp\left[a_1 F \frac{(Vm-V)}{RT}\right]$ (4)

Flux of hydrogen ions H^+, $J_{H+} = \frac{i2}{F} = \frac{i02\ x\ [\text{H+}]}{F} \exp\left[a_2 F \frac{(Vm-V)}{RT}\right]$ (5)

where $io1 = 2.7 \times 10^{11} A\ m^{-2}$

i. $io2 = 2 \times 10^{7} A\ m\ mol^{-1}$
ii. $a_1 = 1$
iii. $a_2 = 0.5$
iv. F = Faraday's constant (96485 C mol^{-1})
v. R = gas constant

3. Results

This section discusses the results obtained from the findings from all computed corrosion models in the study. Two points from the model were taken to be analysed which are represented by Point 5, situated at the mouth of pit, and Point 6, situated at the bottom of the pit.

The magnitude of the current density changes significantly depending on the size of the applied voltage. Figure 2 below shows the polarization curve of the three-dimensional model for pH 8 model.

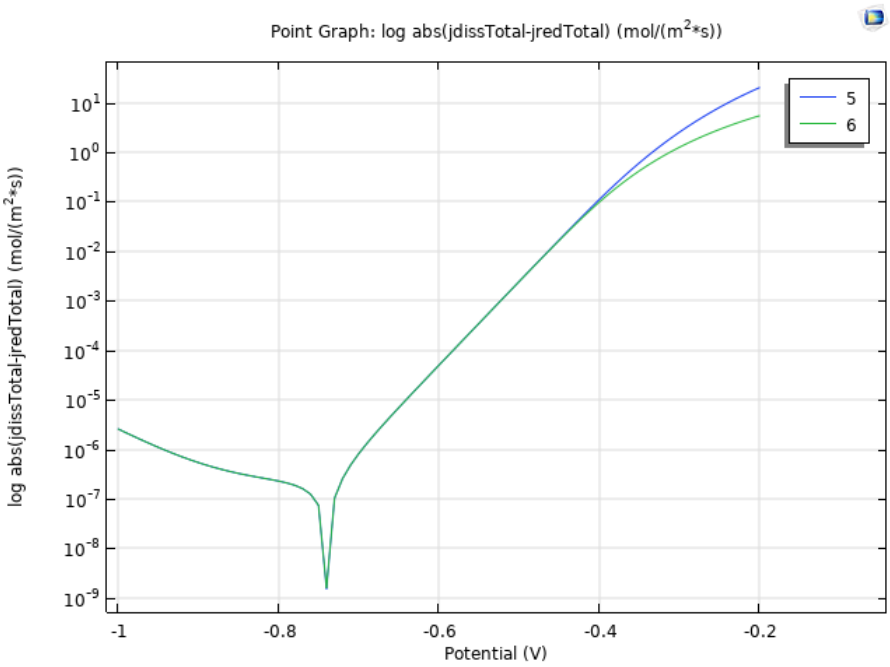

Fig. 2. Polarization curve of pH 8

While Figure 3 is the Evans diagram showing graphical representation of anodic and cathodic polarization. The polarization curve demonstrates that the cathodic reaction predominates at very low potentials. As the potential increases, the cathodic current which represents the reduction process, decreases. Both the anodic and cathodic currents follow Tafel's Law. Hence, when these currents are plotted on a logarithmic axis, the resulting graph is a straight line. The intersection points of the anodic (oxidation) current and the cathodic (reduction) current is the potential at which the equilibrium between anodic and cathodic processes occurs, and this is the corrosion potential, E_{corr}. Corrosion potential indicates the mixed potential at which the rate of anodic dissolution of the electrode is equal to the rate of cathodic reactions. This potential is the tendency of metals to corrode [14]. At this potential, the total current density is zero. The corrosion current density, i_{corr}, can also be obtained at this intersection of anodic and cathodic polarization curve. It can be produced by extrapolating the linear portions of anodic and cathodic lines. From the Evans diagram in Figure 3, the E_{corr} value is -0.74V and the corrosion current density (log i_{corr}) value is measured to be less than 10^{-6} Am^{-2} and this is in line with published result [6]. The polarization curve obtained showed that at low potentials, cathodic reactions dominated the whole process. The cathodic current densities decreased as it reaches the corrosion potential, E_{corr}, at -0.74V. Anodic process dominated as the corrosion activity passed the corrosion potential, resulting in an increase in concentration of Fe^{2+}. A significant difference in the current densities at Point 5 and 6 can be observed starting from -0.4 V. This indicates that corrosion rate at Point 5 is higher compared to Point 6, which may lead to open-mouthed pit shape or general corrosion [7].

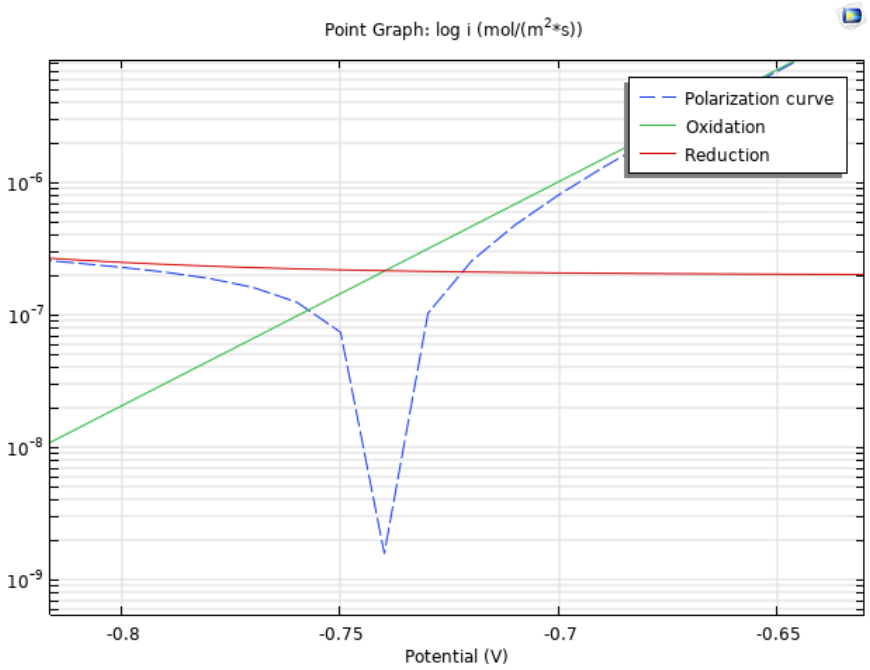

Fig. 3. 1 Evans diagram of pH 8

The increase in current density against potential indicates the occurrence of corrosion activities. Figure 4 shows the cross section of the three-dimensional model showing accumulation of ferrous ions inside the pit, with the bulk solution remains unchanged. This level of Fe^{2+} concentration is significantly high, reaching to 2.5×10^{3} mol m^{-3}, shows that active corrosion is occurring continuously inside the pit.

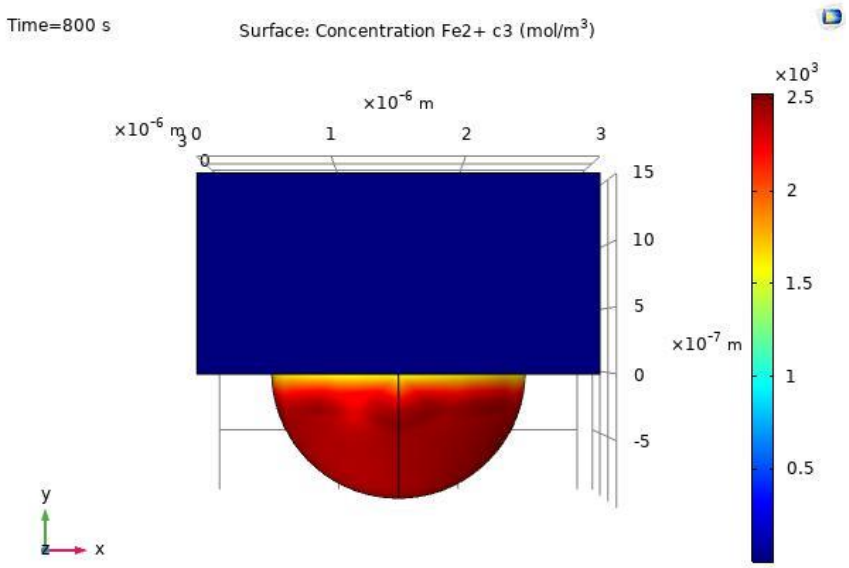

Fig. 4. Fe^{2+} concentration at -0.2V

However, it can be observed that there exists a gradient in the Fe^{2+} concentration at the mouth of the pit compared to that at the bottom of the pit. This is shown in Figure 5 below where there is a significant difference in the level of Fe^{2+} concentrations between the point at the mouth and at the bottom of the pit. The accumulation of metal ions at bottom of the pit is due to diffusion-limited transport. The Fe^{2+} ions can act as a cathode, attracting electrons from the surrounding metal surface

and driving further corrosion. This predicts the pit geometry to be deeper and suggests the first stage of pitting corrosion [7].

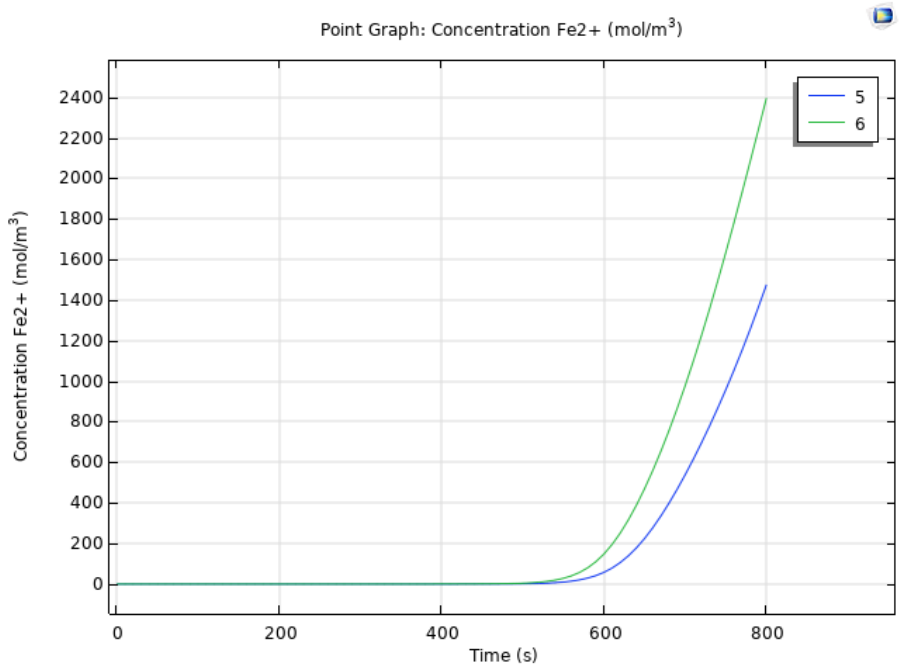

Fig. 5. Fe^{2+} concentration 0-800 seconds

Figure 6 shows the concentration profile of the eleven species applied in the model [15]. This figure illustrates the concentration of all ionic species throughout the process at Point 6. As soon as the Fe^{2+} concentration increases, hydrolyses occurs and with the presence of water, produces $FeOH^{+}$ and H^{+} in the surrounding solution. Production of these species causes the pH solution to reduce and becoming acidic. The concentration of Fe^{2+} is highly increasing inside the pit. Hence, the positively charged ionic species attracts the negatively charged chloride ions, Cl^{-}, into the pit. This occurs through the process of ion migration, which in turn, maintain the electroneutrality of ionic species. Meanwhile the ionic species $FeCl^{+}$ is formed by the reaction between Fe^{2+}+ and Cl- ions. From the figure, it can be related that as Fe^{2+} concentration level starts to increase at potential -0.9 V, and the concentration of $FeOH^{+}$ and $FeCl^{+}$ are also increasing along the process. Around potential of -0.9V, the concentration level of Fe^{2+} starts to increase slowly with the increasing potential. This happens because of the change in the concentration of the electrolyte. At this stage, the electrochemical process is regulated by the rate of mass transfer which is called concentration polarization. The amount of Fe^{2+} discharge from the electrode is balanced by the high level of chloride, so that the charge of ionic species balance is maintained. It can also be observed that the high concentration of Cl^{-} inside the pit is due to the migration of Cl^{-} from bulk solution to the anodic surface area [16]. Thus, Fe^{2+} and Cl^{-} concentration rise slowly as the potential and current density increase. At this stage, it is concluded that this study was able to show the capability of the three-dimensional model to present the change in ionic species concentration against the potential and time taken.

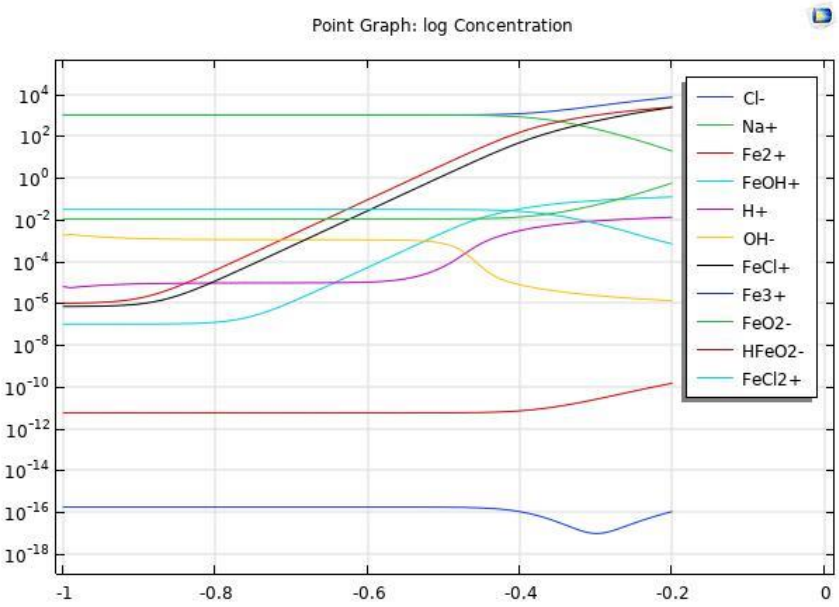

Fig. 6. Concentration profile of 11 ionic species

Figure 7 below shows an illustration of the three-dimensional model of corrosion model at pH 8 environment at 800s, which is at potential -0.2V. At this potential, the upper part of geometry, which is the inactive region, has pH that remain unchanged which is pH 8. At the active part, which is the lower part (pit shape), the pH decreases reaching to pH 5 which indicates acidic environment. [17]. The presence of chloride ions, together with a significant drop in pH inside the pit [16] indicates the first stage of pitting corrosion, as in published model [7].

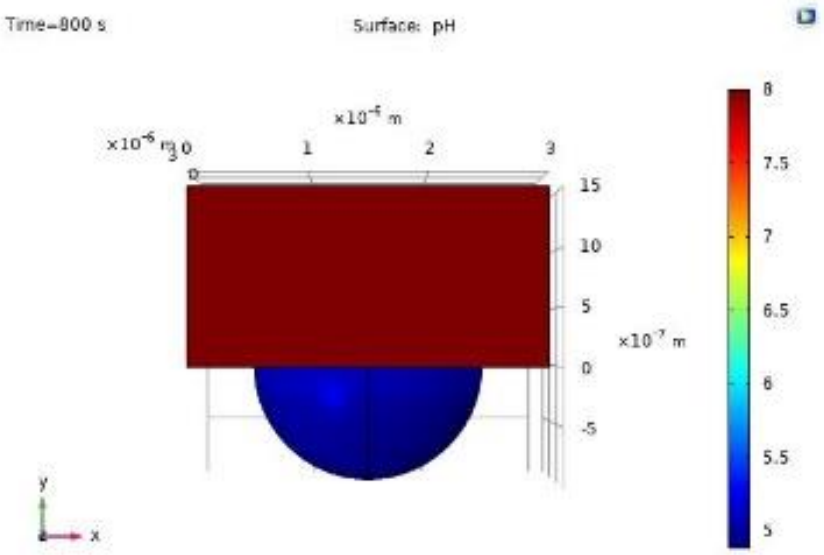

Fig. 7. Three-dimensional model of corrosion model at pH 8 environment at 800s

The pitting behaviour in alkaline solutions was found to be significantly different from that in neutral and acidic solutions [17]. Electrochemical results and SEM images indicate that the product film formed on the metal surface results in different corrosion behaviour in an alkaline solution. SEM

images show that pH and chloride concentration in the bulk solution have a great influence on the pitting morphology [17,18].

This simulation work is validated through published work. Malik *et al.,* stated that at low pH, high Cl^- content and stagnancy are the conditions most suitable for initiation and propagation of pitting [19]. This is in line with this simulation study, where results had shown that chloride plays an important role for the pitting corrosion of steel. In addition, at low chloride concentration, steel remains passive and passivity breakdown started to occur at higher sodium chloride concentration of more than 1 M, as stated by Qiu *et al.,* [20], which is applied in the initial concentration of chloride ions in this model. The passivity breakdown is indicated by the polarization curve produced in this modelling work with E_{corr} -0.74V. This is also supported by the work done by Parangusan *et al.,* [21], which stated that aggressive chloride ions react with the metal ions and cause metal dissolution. In addition, Parangusan *et al.,* have studied different initial pH, which shifted the values of E_{corr} respectively. As a recommendation, future work should focus on the results when the model is solved at a higher potential with different initial pH of the surrounding solution.

4. Conclusion

This study was devoted to show the capability of the three-dimensional model to present the propagation of corrosion on steel surface for a range of potential. Simulations were carried out to solve Nernst-Planck equations of eleven ionic species by using COMSOL Multiphysics software with Chemical Reaction Engineering Module as a tool, applied in the three-dimensional corrosion model with initial pH 8 chloride solution. Data from the software is presented in line graphs and model image geometries to present the ionic species concentration level. The model showed evidence that at a higher potential, the model can present more corrosion activities relating to pitting corrosion. A polarization curve, indicating the occurrence of metal dissolution, with corrosion potential -0.74 V was obtained and the pH value at the bottom of the pit turns acidic and reached pH 4.9 after running the model for potential range -1.0 until -0.2 V. This change in pH indicates the occurrence of pitting corrosion. Meanwhile, the concentration of Fe^{2+} reached $2.53x10^3$ mol/m^3 which indicates metal loss into the bulk solution. Comparisons were made and the results are in line with the Pourbaix diagram of iron, as well as between the experimental findings and published models. This research has achieved its target which a three-dimensional model in chloride-induced environment with slightly alkaline pH has successfully been simulated to obtain its corrosion behaviour.

Acknowledgement

This study is funded by the Ministry of Higher Education (MOHE) of Malaysia through the Fundamental Research Grant Scheme (FRGS), No: FRGS/1/2018/STG06/UTEM/02/2. The authors would also like to thank Universiti Teknikal Malaysia Melaka (UTeM) for all the support given.

References

[1] Ansari, Talha Qasim, Jing-Li Luo, and San-Qiang Shi. "Modeling the effect of insoluble corrosion products on pitting corrosion kinetics of metals." *npj Materials Degradation* 3, no. 1 (2019): 28. https://doi.org/10.1038/s41529-019-0090-5

[2] How, Heoy Geok, Justine Wei Sze Hwang, Yew Heng Teoh, Hun Guan Chuah, Jason Jun Jie Yeoh, and Jun Sheng Teh. "Investigation of the corrosion metals in moringa biodiesel fuel." *Journal of Advanced Research in Fluid Mechanics and Thermal Sciences* 75, no. 1 (2020): 94-103. https://doi.org/10.37934/arfmts.75.1.94103

[3] Huang, Haijia, Chen Jia, and Lanhui Guo. "Effect of local corrosion on tensile behavior of steel plates." In *Structures*, vol. 43, pp. 977-989. Elsevier, 2022. https://doi.org/10.1016/j.istruc.2022.07.027

[4] Reda, Y., A. M. El-Shamy, K. M. Zohdy, and Ashraf K. Eessaa. "Instrument of chloride ions on the pitting corrosion of electroplated steel alloy 4130." *Ain Shams Engineering Journal* 11, no. 1 (2020): 191-199. https://doi.org/10.1016/j.asej.2019.09.002
[5] Fontana, M. G. "Corrosion Engineering 3rd edition McGraw-Hill Book Company." (1987): 39-60.
[6] Narayanan, Deeparekha, Lin Chen, Bilal Mansoor, and Homero Castaneda. "A new insight into pitting initiation in selective laser melted 316L stainless steel." *Materials Letters* 333 (2023): 133562. https://doi.org/10.1016/j.matlet.2022.133562
[7] Salleh, Suhaila. *Modelling pitting corrosion in carbon steel materials*. The University of Manchester (United Kingdom), 2013.
[8] Verma, Eshaan, Harshal Gajera, Dharam Ramani, Namrata Bist, and Anirbid Sircar. "Corrosion in the light of electrochemistry." *Materials Today: Proceedings* 62 (2022): 7057-7061. https://doi.org/10.1016/j.matpr.2022.01.138
[9] Ma, Heng, Zhong-xue Wang, Yue Liu, Yue-xiang Wang, Teng-fei Wang, Qing-pu Zhang, and Zhong-yu Cui. "pH-dependent corrosion initiation behavior induced by inclusions of low alloy steel in simulated marine environments." *Journal of Iron and Steel Research International* (2022): 1-13. https://doi.org/10.1007/s42243-022-00878-1
[10] Turnbull, A., and M. K. Gardner. "Electrochemical polarization studies of BS 4360 50D steel in 3.5% NaCl." *Corrosion Science* 22, no. 7 (1982): 661-673. https://doi.org/10.1016/0010-938X(82)90046-4
[11] Perez, Nestor, and Nestor Perez. "Electrochemical corrosion." *Electrochemistry and Corrosion Science* (2016): 1-23. https://doi.org/10.1007/978-3-319-24847-9_1
[12] Meng, Da, Bin Zheng, Guang Lin, and Maria L. Sushko. "Numerical solution of 3D Poisson-Nernst-Planck equations coupled with classical density functional theory for modeling ion and electron transport in a confined environment." *Communications in Computational Physics* 16, no. 5 (2014): 1298-1322. https://doi.org/10.4208/cicp.040913.120514a
[13] Turnbull, A., and D. H. Ferriss. "Mathematical modelling of the electrochemistry in corrosion fatigue cracks in steel corroding in marine environments." *Corrosion Science* 27, no. 12 (1987): 1323-1350. https://doi.org/10.1016/0010-938X(87)90129-6
[14] Papavinasam, Sankara. "Electrochemical polarization techniques for corrosion monitoring." In *Techniques for corrosion monitoring*, pp. 45-77. Woodhead Publishing, 2021. https://doi.org/10.1016/B978-0-08-103003-5.00003-5
[15] Mortadha, Noor Mirza Syamimi, Suhaila Salleh, and Alzakri Ekhwan. "3D modelling of localized corrosion in steel using COMSOL multiphysics." *Proceedings of Mechanical Engineering Research Day 2022* 2022 (2022): 156-157.
[16] Alamri, Aeshah H. "Localized corrosion and mitigation approach of steel materials used in oil and gas pipelines–An overview." *Engineering failure analysis* 116 (2020): 104735. https://doi.org/10.1016/j.engfailanal.2020.104735
[17] Wang, Yafei, Guangxu Cheng, Wei Wu, Qiao Qiao, Yun Li, and Xiufeng Li. "Effect of pH and chloride on the micro-mechanism of pitting corrosion for high strength pipeline steel in aerated NaCl solutions." *Applied Surface Science* 349 (2015): 746-756. https://doi.org/10.1016/j.apsusc.2015.05.053
[18] Hou, Xianglong, Quanyou Ren, Youkun Yang, Xianlong Cao, Jie Hu, Cheng Zhang, Hongda Deng, Daliang Yu, Kejian Li, and Wei Lan. "Effect of temperature on the electrochemical pitting corrosion behavior of 316L stainless steel in chloride-containing MDEA solution." *Journal of Natural Gas Science and Engineering* 86 (2021): 103718. https://doi.org/10.1016/j.jngse.2020.103718
[19] Malik, A. U., PC Mayan Kutty, Nadeem A. Siddiqi, Ismaeel N. Andijani, and Shahreer Ahmed. "The influence of pH and chloride concentration on the corrosion behaviour of AISI 316L steel in aqueous solutions." *Corrosion science* 33, no. 11 (1992): 1809-1827. https://doi.org/10.1016/0010-938X(92)90011-Q
[20] Qiu, Jie, Yakun Zhu, Yi Xu, Yanhui Li, Feixiong Mao, Angjian Wu, and Digby D. Macdonald. "Effect of chloride on the pitting corrosion of carbon steel in alkaline solutions." *Journal of The Electrochemical Society* 169, no. 3 (2022): 031501. https://doi.org/10.1149/1945-7111/ac580c
[21] Parangusan, Hemalatha, Jolly Bhadra, and Noora Al-Thani. "A review of passivity breakdown on metal surfaces: Influence of chloride-and sulfide-ion concentrations, temperature, and pH." *Emergent Materials* 4, no. 5 (2021): 1187-1203. https://doi.org/10.1007/s42247-021-00194-6